

Synthesis and some properties of 14 group element-containing alkylidene complexes of molybdenum and tungsten

Leonid N. Bochkarev *, Yulia E. Begantsova, Vladislav I. Shcherbakov, Natalia E. Stolyarova, Irina K. Grigorieva, Irina P. Malysheva, Galina V. Basova, Andrey L. Bochkarev, Yulia P. Barinova, Georgii K. Fukin, Evgenii V. Baranov, Yurii A. Kurskii, Gleb A. Abakumov

G.A. Razuvaev Institute of Organometallic Chemistry, Russian Academy of Sciences, Russian Federation, Tropinina 49, Nizhny Novgorod 603950, Russia

Received 30 May 2005; accepted 8 July 2005

Available online 30 August 2005

Abstract

Alkylidene complex of molybdenum $\text{Ph}_3\text{Si}-\text{CH}=\text{Mo}(\text{NAr})(\text{OCMe}_2\text{CF}_3)_2$ (**1**) ($\text{Ar} = 2,6\text{-Pr}_2\text{C}_6\text{H}_3$) has been prepared by the reaction of $\text{Ph}_3\text{SiCH}=\text{CH}_2$ with known alkylidene compounds $\text{Alkyl}-\text{CH}=\text{Mo}(\text{NAr})(\text{OCMe}_2\text{CF}_3)_2$ ($\text{Alkyl} = \text{Bu}^t, \text{PhMe}_2\text{C}$). According to X-ray diffraction studies the geometry of the Mo atom in (**1**) can be described as a distorted tetrahedron. Reactions of heteroelement-containing imido alkyl compounds of molybdenum and tungsten $(\text{ArN})_2\text{M}(\text{CH}_2\text{EMe}_3)_2$ ($\text{Ar} = 2,6\text{-Pr}_2\text{C}_6\text{H}_3$; $\text{M} = \text{Mo}, \text{W}$; $\text{E} = \text{Si}, \text{Ge}, \text{Sn}$) with triflic acid were shown to yield a complex mixture of products among which carbene complexes have not been observed. The formation of carbene complexes of tungsten in low yields was observed by ^1H NMR spectroscopy in the reactions of $(\text{ArN})_2\text{W}(\text{CH}_2\text{EMe}_3)_2$ ($\text{E} = \text{Si}, \text{Ge}, \text{Sn}$) with hydrogen chloride in $\text{THF}-d_8$. Catalytic properties of heteroelement-containing alkylidene complexes of molybdenum $\text{R}_3\text{E}-\text{CH}=\text{Mo}(\text{NAr})(\text{OCMe}_2\text{CF}_3)_2$ ($\text{E} = \text{Si}, \text{Ge}$; $\text{R} = \text{Me}, \text{Ph}$) and also hydrocarbon analogs $\text{Alkyl}-\text{CH}=\text{Mo}(\text{NAr})(\text{OCMe}_2\text{CF}_3)_2$ ($\text{Alkyl} = \text{Bu}^t, \text{PhMe}_2\text{C}$) in metathesis of 1-hexene were investigated. The catalytic activity of alkylidene complexes was shown to depend essentially on the nature of substituent bonded to carbene carbon atom.

© 2005 Elsevier B.V. All rights reserved.

Keywords: Alkylidene complexes; Molybdenum; Tungsten; Silicon; Germanium; Tin; Synthesis; Structure elucidation; Olefin metathesis; Catalytic activity

1. Introduction

We have recently reported the synthesis of germanium-containing alkylidene complexes of molybdenum $\text{R}_3\text{Ge}-\text{CH}=\text{Mo}(\text{NAr})(\text{OCMe}_2\text{CF}_3)_2$ ($\text{R} = \text{Me}, \text{Ph}$) [1] prepared by the reaction of organogermanium vinyl reagents $\text{R}_3\text{Ge}-\text{CH}=\text{CH}_2$ with known alkylidene compounds $\text{Alkyl}-\text{CH}=\text{Mo}(\text{NAr})(\text{OCMe}_2\text{CF}_3)_2$ ($\text{Alkyl} = \text{Bu}^t,$

PhMe_2C). The reaction was originally developed by Schrock and co-workers for preparation of trimethylsilyl-containing carbene compounds of molybdenum and tungsten [2].

Herein we report the synthesis by the above method of the triphenylsilyl-containing complex (**1**). The results of attempted preparation of heteroelement-containing carbene complexes of molybdenum and tungsten by reactions of imido alkyl compounds $(\text{ArN})_2\text{M}(\text{CH}_2\text{-EMe}_3)_2$ ($\text{M} = \text{Mo}, \text{W}$; $\text{E} = \text{Si}, \text{Ge}, \text{Sn}$) with triflic acid and hydrogen chloride are reported and discussed as well. Catalytic properties of a series of silicon- and

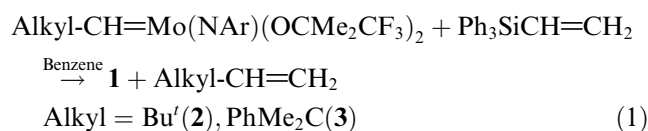
* Corresponding author. Tel.: +7 8312 12 7010; fax: +7 8312 12 7497.

E-mail address: lnb@imoc.sinn.ru (L.N. Bochkarev).

germanium-containing carbene complexes of molybdenum $R_3E-CH=Mo(NAr)(OCMe_2CF_3)_2$ ($E = Si, Ge$; $R = Me, Ph$) and also hydrocarbon analogs $Alkyl-CH=Mo(NAr)(OCMe_2CF_3)_2$ ($Alkyl = Bu^t, PhMe_2C$) in metathesis of 1-hexene have been studied.

2. Results and discussion

The reactions of $Alkyl-CH=Mo(NAr)(OCMe_2CF_3)_2$ ($Alkyl = Bu^t$ (**2**), $PhMe_2C$ (**3**)) with $Ph_3Si-CH=CH_2$ were found to proceed much more slowly than the analogous reactions with $Me_3Si-CH=CH_2$ [2a] and $R_3Ge-CH=CH_2$ [1] and to complete in 2 months at room temperature (Eq. (1)):



The course of the reactions was monitored by 1H NMR. In contrast to previously studied similar reactions of compounds **2** and **3** with organogermanium vinyl reagents [1] the following interesting changes were observed in the H_α region. Just after the mixing of the reagents besides of the resonance at 11.61 ppm ($J_{HC} = 119.4$ Hz) of the H_α of the starting compound **2** [2a] an additional signal at 11.16 ($J_{HC} = 137.0$ Hz) ppm was observed. The ratio of the signals was $\approx 6:1$. The following reaction led to the decreasing of the intensities of the initial signals at 11.61 and at 11.16 ppm and appearing the signals at 13.29 ppm and at 12.87 ppm with $\approx 2:1$ ratio of the forming complex **1**. After the completion of the reaction the signals at 11.61 and at 11.16 ppm were disappeared completely and the signals at 13.29 and at 12.87 ppm were increased and remained with the ratio $\approx 2:1$. The similar transformations were observed in the reaction with **3** as a starting compound. We propose that the minor signal at 11.16 ppm with the larger J_{HC} coupling constant (137.0 Hz) is related to *anti* rotamer of the initial compound **2** and is unusually located upfield from the major signal of the *syn* rotamer (11.61 ppm, $J_{HC} = 119.4$ Hz [2a]). *Syn-anti* interconversion of alkylidene complexes is well known [3] and the larger J_{HC} coupling constants (usually about 140 Hz) for *anti* rotamers in comparison to *syn* rotamers (usually about 125 Hz) is a characteristic feature for a wide variety of molybdenum and tungsten alkylidene compounds [3]. However, we have not yet a reasonable explanation why just addition of silicon-containing vinyl reagent in contrast to germanium-containing vinyl reagents has led to *syn-anti* interconversion of the starting compound **2**. The J_{HC} coupling constants for H_α signals have not been observed in the 1H NMR spectrum of the product **1**. The J_{CH} coupling constants – $J_{CH} = 112.4$ Hz (δ , 261.1 ppm) and $J_{CH} = 112.9$ Hz

(δ , 256.6 ppm) – observed in ^{13}C MNR spectrum of product **1** are almost equal. Therefore, we can only propose on the basis of signal intensities (typically a *syn* isomer has a major signal [3]) that the resonances at 13.29 ppm and at 12.87 ppm are in the 1H NMR spectrum are related, respectively, to *syn* and *anti* rotamers of the formed complex **1**.

The molybdenum alkylidene complex **1** was isolated as air-sensitive yellow-orange crystalline solid. It was characterized by elemental analysis, 1H NMR, ^{13}C NMR spectroscopy. The structures of **1** known compound $Me_3Si-CH=Mo(NAr)(OCMe_2CF_3)_2$ (**4**) were determined by X-ray diffraction studies. According to X-ray data the complexes **1** and **4** have a *syn*-conformation. The Mo and Si atoms have a typical tetrahedral coordination environment (Figs. 1 and 2). The Mo(1)–N(1)C(1) (in **1**) and Mo(1)N(1)C(13) (in **4**) angles in diisopropylphenylimido ligands are equal to $174.8(2)^\circ$ and $168.3(1)^\circ$, respectively. It should be noted that the coordinating environments of Mo and Si atoms in **1**, **4** are quite similar to coordinating environments of Mo and Ge atoms in $R_3Ge-CH=Mo(NAr)(OCMe_2CF_3)_2$ ($R = Me, Ph$) complexes [1]. The Mo(1)–N(1) distances are 1.725(2) and 1.722(2) Å for **1** and **4**, respectively. The geometries of the MoCSi fragments are slightly different in **1** and **4**. The main difference is observed in the values of MoCSi angles. In more bulky **1**, the Mo(1)C(21)Si(1) ($144.8(2)^\circ$) angle is significantly larger than the analogous value in **4** ($138.5(1)^\circ$). The similar situation is observed in $R_3Ge-CH=Mo(NAr)(OCMe_2CF_3)_2$ ($R = Me, Ph$) complexes [1]. The Mo=C(SiR₃) distances are close to each other (1.883(3) Å in **1**, 1.889(2) Å in **4**) and to the values of Mo=C(GeR₃) distances (1.876(2) Å for $R = Ph$ and 1.889(2) Å for $R = Me$ [1]).

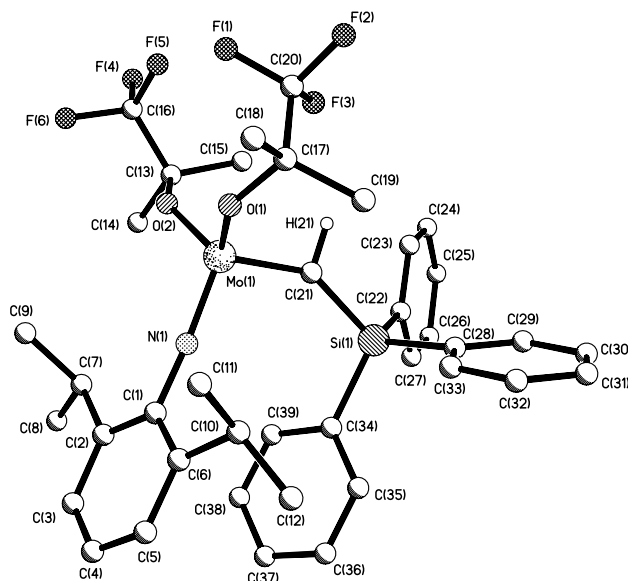
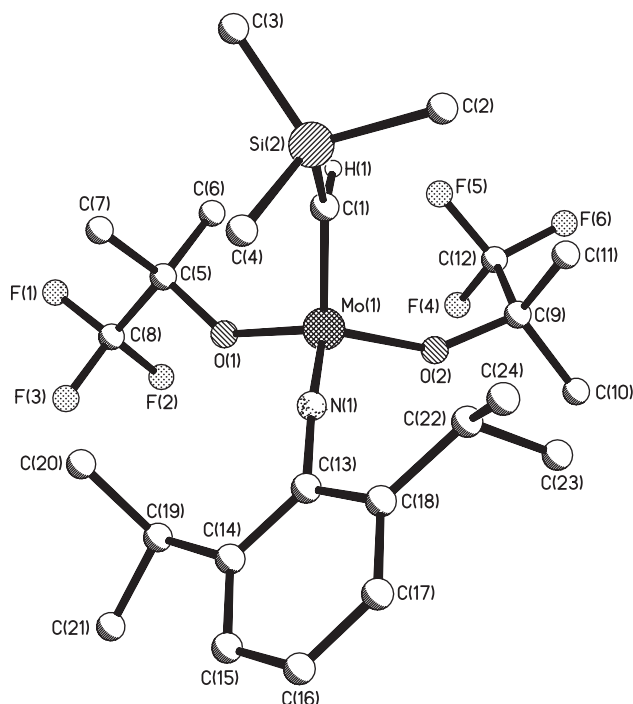
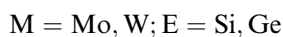
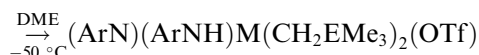


Fig. 1. Molecular structure of **1**.

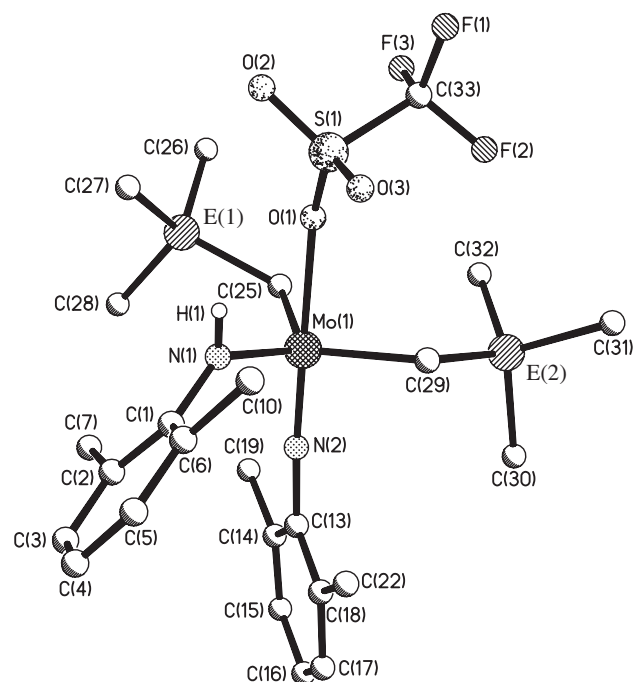
Fig. 2. Molecular structure of **4**.

Although the reactions of alkylidene compounds **2** and **3** with organosilicon or organogermanium vinyl reagents allowed to obtain heteroelement-containing carbene complexes of molybdenum, this method seemed to us somewhat inconvenient due to the multistep synthesis of the starting materials. Therefore, we attempted the synthesis of heteroelement-containing carbene complexes of molybdenum and tungsten by the reactions of silicon-, germanium- and tin-containing imido alkyl compounds $(\text{ArN})_2\text{M}(\text{CH}_2\text{EMe}_3)_2$ ($\text{Ar} = 2, 6\text{-Pr}_2\text{C}_6\text{H}_3$; $\text{M} = \text{Mo}, \text{W}$; $\text{E} = \text{Si}, \text{Ge}, \text{Sn}$) [4,5] with triflic acid and hydrogen chloride. This method was successfully used for preparation of hydrocarbon imido alkylidene compounds of the type $\text{Alkyl-CH}=\text{M}(\text{NAr})(\text{OTf})_2(\text{DME})$ ($\text{M} = \text{Mo}, \text{W}$; $\text{Alkyl} = \text{Bu}^t, \text{PhMe}_2\text{C}$) [2b,6].

The reactions of $(\text{ArN})_2\text{M}(\text{CH}_2\text{EMe}_3)_2$ ($\text{M} = \text{Mo}, \text{W}$; $\text{E} = \text{Si}, \text{Ge}, \text{Sn}$) with 3 equiv. of triflic acid in DME at -50°C followed with slow warming to room temperature led to the formation of amido imido compounds $(\text{ArN})(\text{ArNH})\text{M}(\text{CH}_2\text{EMe}_3)_2(\text{OTf})$ (20–30%), anilinium salt (15–20%), Me_4E (15–20%) and some unidentified products. Carbene complexes have not been observed in the reaction mixtures. Amido imido compounds are obviously the products of the first stage of the reactions. To confirm this we showed that the reactions of imido alkyl compounds with 1 equiv. of triflic acid yielded the amido imido compounds as the major products (Eq. (2)):



(2)

Fig. 3. Molecular structure of **5** ($\text{E} = \text{Si}$) and **6** ($\text{E} = \text{Ge}$). (The carbon atoms at C(7), C(10) and C(19), C(22) are omitted for clarity.)

Complexes $(\text{ArN})(\text{ArNH})\text{Mo}(\text{CH}_2\text{SiMe}_3)_2(\text{OTf})$ (**5**), $(\text{ArN})(\text{ArNH})\text{Mo}(\text{CH}_2\text{GeMe}_3)_2(\text{OTf})$ (**6**), $(\text{ArN})(\text{ArNH})\text{W}(\text{CH}_2\text{GeMe}_3)_2(\text{OTf})$ (**7**) were isolated in 60–80% yields as air-sensitive orange (Mo) or pale green (W) crystalline solids. They were identified by elemental analysis, ^1H , ^{13}C , ^{29}Si NMR spectroscopy. According to X-ray analysis the Mo atoms in compounds **5** and **6** have a distorted trigonal-bipyramidal coordination with $\text{CH}_2\text{-EMe}_3$, ArNH ligands in the equatorial plane, whereas ArN and OTf groups are apical positioned (Fig. 3). The $\text{Mo}(1)\text{-N}(1)$ distances and $\text{Mo}(1)\text{N}(1)\text{C}(1)$, $\text{Mo}(1)\text{N}(2)\text{C}(13)$ angles are close to each other (1.925(5) Å and $138.2(4)^\circ$, $174.8(4)^\circ$ in **5**; 1.917(2) Å and $136.3(1)^\circ$, $175.6(2)^\circ$ in **6**) except for the bond lengths $\text{Mo}(1)\text{-N}(2)$ which are distinctly different (1.716(4) Å in **5** and 1.748(1) Å in **6**). The $\text{Mo}(1)\text{-O}(\text{Tf})$ distances are also different (2.214(4) Å in **5** and 2.243(1) Å in **6**) in contrast to the equal bond lengths $\text{Mo-O}(\text{CMe}_2\text{CF}_3)$ in **1**, **4** (1.901(1)–1.906(1) Å). The $\text{Mo}(1)\text{-C}(\text{EMe}_3)$ distances in **5**, **6** vary in the narrow range of 2.091(5)–2.104(2) Å. The MoCE bond angles ($115.9(1)$ – $126.8(3)^\circ$) are somewhat bigger than the typical values for sp^3 carbon atoms.

Similar chloro-containing amido imido complexes of tungsten $(\text{ArN})(\text{ArNH})\text{W}(\text{CH}_2\text{EMe}_3)_2(\text{Cl})$ ($\text{E} = \text{Si}$ (**8**), Ge (**9**)) were isolated in 30–35% yields in the reactions of $(\text{ArN})_2\text{W}(\text{CH}_2\text{EMe}_3)_2$ ($\text{E} = \text{Si}, \text{Ge}$) with 1 equiv. of hydrogen chloride in THF (Eq. (3)):



(3)

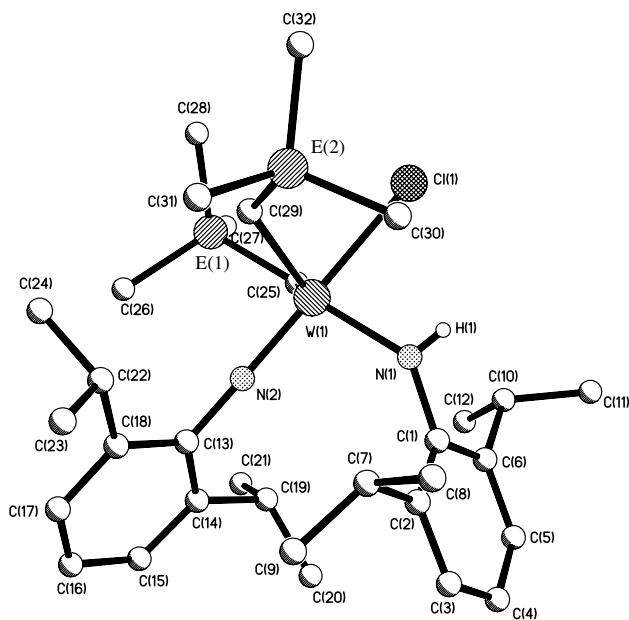


Fig. 4. Molecular structure of **8** (E = Si) and **9** (E = Ge).

Complexes **8** and **9** are unstable in air pale green crystalline solids. They were characterized by elemental analysis, ^1H , ^{13}C NMR spectroscopy and X-ray diffraction studies.

According to X-ray analysis the W atoms in compounds **8** and **9** have a distorted trigonal-bipyramidal coordination. As in **4** and **5**, the equatorial positions occupy CH_2EMe_3 , ArNH ligands. The chlorine atom and amido substituent are located in the apical sites (Fig. 4). The $\text{W}(1)\text{--N}(1,2)$ distances and the values of angles around N(1), N(2) atoms are 1.924(2), 1.755(2) Å and $136.6(1)^\circ$, $176.6(1)^\circ$ for **8** and 1.933(2), 1.745(2) Å and $135.0(1)^\circ$, $176.7(1)^\circ$ for **9**. It should be noted that the geometrical parameters of imido and amido fragments in **8** and **9** are close to the appropriate parameters in Mo-complexes **5** and **6**. The $\text{W}(1)\text{--Cl}(1)$ distances in **8** and **9** (2.4920(5) and 2.4942(6) Å correspondingly) are significantly longer than the respective distances in $\text{Ph}_3\text{E--CH=WCl}_2(\text{O}i\text{Bu}^t)_2$ (E = Si, Ge) (2.373(1)–2.385(1) Å [7]). The bond lengths $\text{W}(1)\text{--C}(25, 29)$ and the values of $\text{W}(1)\text{C}(25, 26)\text{E}(1, 2)$ angles in **8** (2.104(2), 2.112(2) Å; $118.85(9)^\circ$, $125.4(1)^\circ$) and in **9** (2.111(2), 2.093(2) Å; $116.2(1)^\circ$, $122.9(1)^\circ$) are close to those in **5** and **6**. The distances $\text{E}(1)\text{--C}(25)$ and $\text{E}(2)\text{--C}(29)$ are 1.889(2), 1.887(2) Å for **8** and 1.973(2), 1.976(2) Å for **9**. The difference between E–C distances is close to the difference between covalent radii of Si and Ge atoms.

The reactions of tungsten imido alkyl compounds $(\text{ArN})_2\text{W}(\text{CH}_2\text{EMe}_3)_2$ (E = Si, Ge, Sn) with 3 equiv. of hydrogen chloride in $\text{THF-}d_8$ according to ^1H NMR spectroscopy data completed at room temperature within 10–30 min and yielded $(\text{ArN})(\text{ArNH})\text{W}(\text{CH}_2\text{EMe}_3)_2(\text{Cl})$ ($\approx 3\text{--}5\%$), $[\text{ArNH}_3][\text{Cl}]$ ($\approx 3\text{--}5\%$), Me_4E

Table 1
Kinetic data for the metathesis of 1-hexene using molybdenum catalysts^a

Catalyst	Temp (°C)	Conversion (%)	10^4k ($\text{L mol}^{-1} \text{s}^{-1}$)
2	22	40.55	4.77
3	22	30.17	3.22
4	20	13.98	1.14
10	26	19.01	1.73
11	26	7.63	0.35

^a $[\text{1-hexene}]/[\text{catalyst}] = 300$; neat 1-hexene; time of the reaction – 3 min.

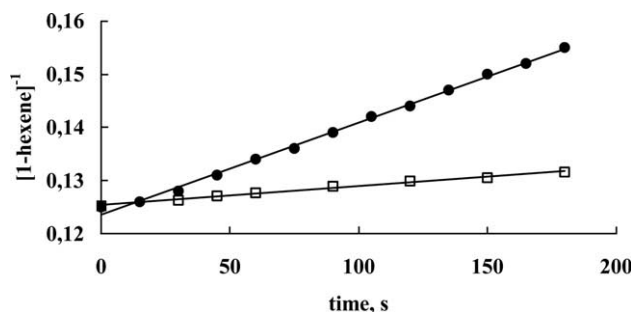
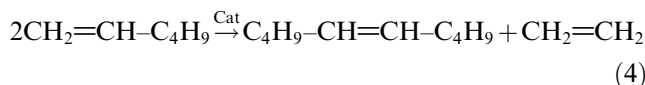


Fig. 5. Second-order kinetic plot for the metathesis of 1-hexene with **10** (●) and **11** (□) as catalysts; $[\text{1-hexene}]_0 = 7.99 \text{ mol L}^{-1}$, $[\text{Cat}] = 0.027 \text{ mol L}^{-1}$ at 26 °C. Kinetic plots for other catalysts **2**, **3** and **4** have a similar second-order character.

($\approx 3\text{--}5\%$), Me_3ECl ($\approx 80\%$), ArNH_2 ($\approx 80\%$), carbene complexes ($\approx 3\text{--}5\%$) of the proposed composition $[(\text{ArN})\text{W}(\text{=CH--EMe}_3)(\text{Cl})_2]$, and some other products with W--CH_3 fragments. The resonance signal of H_α atom in the fragment W=CH--SiMe_3 was found at 11.82 ppm, in the fragment W=CH--GeMe_3 – at 11.81 ppm and in the fragment W=CH--SnMe_3 – at 12.15 ppm downfield from TMS.

Catalytic properties of 14 group element-containing carbene complexes of molybdenum in olefin metathesis reactions have been explored using neat 1-hexene as a testing substrate (Eq. (4)):



The compounds $\text{R}_3\text{Ge--CH=Mo}(\text{NAr})(\text{OCMe}_2\text{CF}_3)_2$ (R = Me (**10**), Ph (**11**)), and **4** were found to reveal high catalytic activity in metathesis of 1-hexene, comparable with catalytic activity of known, one of the most active catalysts **2** and **3** (Table 1, Fig. 5). Comparison of the rate constants presented in Table 1 allows to conclude that germanium- and silicon-containing complexes **10**, **11**, **4** are 2–14 times less active catalysts than hydrocarbon analogs **2** and **3**. The activities of silicon-containing complex **4** and germanium-containing analog **10** do not differ significantly. The activity of the compounds **10**, **11**, **4** depends on the nature of radicals bonded to E

element. Complexes with Me radicals (**10**, **4**) are more active catalysts than complex with Ph radicals (**11**). It is interesting to note that a similar feature was observed for the hydrocarbon analogs **2** and **3**. Complex with Mo=CH–C(CH₃)₃ fragment (**2**) appeared to be somewhat more active than complex with Mo=CH–C(CH₃)₂Ph fragment (**3**). Unfortunately, we could not find in the literature an exact comparable data on activities of compounds **2** and **3** in metathesis of terminal olefins. According [8] when a neopentylidene molybdenum complex Bu^t–CH=Mo(NR)(OR') (R = 2,6-Me₂C₆H₃; R' = CMe(CF₃)₂) and a similar neophylidene complex PhMe₂C–CH=Mo(NR)(OR') were used as catalysts for metathesis of 1-hexene (in methyl cyclohexane as a solvent) a conversion rate was the same.

The rate of olefin metathesis reactions is well known to depend on many factors. The main are the composition and structure of the catalyst, reaction conditions, the nature of the substrate. We found that the rate constants of 1-hexene metathesis were correlated with the steric crowding of the used heteroelement-containing catalysts **4**, **10**, **11**. The sum of ligands solid angles (*Q*, sterad) around Mo atom was selected as a characteristic of molecular structure [9]. The *Q*-value indicates the degree of saturation of the coordination sphere around Mo atom and therefore can serve as a parameter characterizing the steric crowding of molybdenum alkylidene complexes. It should be noted that the *Q* values for **4**, **10** and **11** were calculated from own X-ray data. Unfortunately, the X-ray data for the complexes **2** and **3** are absent. The *Q* values for **10**, **4** and **11** are equal 11.39, 11.42 and 11.73 sterad, respectively (full coordination sphere is 4π sterad). The increase of *Q* values for heteroelement-containing catalysts in the row **10** < **4** < **11** is in accordance with the decrease of the rates of metathesis of 1-hexene using these catalysts in the same order.

3. Experimental

3.1. General

All manipulations were carried out in evacuated sealed ampoules using standard Schlenk techniques. The solvents were thoroughly dried and degassed. Compounds **2** and **3** [2a] and Ph₃SiCH=CH₂ [10] were prepared according to a literature procedure. ¹H, ¹³C, ²⁹Si NMR spectra were recorded on a Bruker DPX-200 NMR spectrometer. NMR data are listed in parts per million downfield from TMS. GLC analysis of metathesis products were performed on "Tsvet-800" gas chromatograph with a 0.3 × 300 cm stainless-steel column filled with SE-30 (5%) on Inerton AW (with katharometer as a detector and helium as the carrier gas).

3.2. Preparation of Ph₃Si–CH=Mo(NAr)(OCMe₂–CF₃)₂ (**1**)

A solution of Ph₃SiCH=CH₂ (0.135 g, 0.48 mmol) in 2 mL of benzene was added to a solution of **2** (0.28 g, 0.48 mmol) in 3 mL of benzene. The reaction mixture was kept at room temperature for 2 months. Evaporation of the solvent and volatiles in vacuo and crystallization of the solid residue from pentane (2 mL) afforded 0.17 g (45%) of **1** as yellow-orange crystals. Anal. Calc. for C₃₉H₄₅F₆SiMoNO₂: C, 58.71; H, 5.70. Found: C, 58.62; H, 5.64%. ¹H NMR (200 MHz, C₆D₆) δ 13.29 and 12.87 (s, 1H, MoCHSiPh₃), 7.74–6.86 (m, 18H, H_{arom}), 3.56 (sept, 2H, CHMe₂, ³J_{HH} = 6.8), 1.35 and 1.23 (s, 6H each, OCMe₂CF₃), 1.06 (d, 12H, CHMe₂). ¹³C NMR (50 MHz, C₆D₆) δ 261.1 (*J*_{CH} = 112.4 Hz) and 256.6 (*J*_{CH} = 112.9 Hz) (MoCHSiPh₃), 154.0, 145.7, 136.3, 135.7, 129.8, 128.3 (C_{arom}), 127.0 (q, ¹J_{CF} = 285.6, OCMe₂CF₃), 122.8 (C_{arom}), 79.7 (q, ²J_{CF} = 28.8, OCMe₂CF₃), 24.9 (CHMe₂), 24.6 and 24.5 (CHMe₂), 23.7 (OCMe₂CF₃). The reaction of Ph₃SiCH=CH₂ with **3** was carried out in a similar way. The yield of **1** was 55%.

3.3. Preparation of (ArN)(ArNH)Mo(CH₂SiMe₃)₂–(OTf) (**5**)

To a dark red solution of (ArN)₂Mo(CH₂SiMe₃)₂ (0.58 g, 0.93 mmol) in 15 ml of DME at –50 °C 0.14 g (0.93 mmol) of HOTf was added. The reaction mixture was stirred and allowed to warm slowly to room temperature. The solution became bright orange-red. The solvent was removed in vacuo. The solid residue was recrystallized from minimal amount of ether to afford orange crystals of **5** 0.6 g (83.3%). Anal. Calc. for C₃₃H₅₇F₃MoN₂O₃SSi₂: C, 51.36; H, 7.39. Found: C, 51.40; H, 7.44%. ¹H NMR (200 MHz, C₆D₆) δ 9.39 (s, 1H, NH), 7.10–6.70 (m, 6H, H (3,4)), 3.66 (d, 2H, MoHCHSiMe₃, ²J_{HH} = 9.0), 3.63 (sept, 2H, CHMe₂), 3.52 (sept, 2H, CHMe₂), 2.35 (d, 2H, MoHCHSiMe₃, ²J_{HH} = 9.0), 1.00 (d, 24H, CHMe₂, ³J_{HH} = 6.8), 0.24 (s, 18H, SiMe₃). ¹³C NMR (50 MHz, C₆D₆) δ 150.81, 149.06, 142.87, 131.19, 127.29, 124.18, 123.95 (C_{arom}); 75.42 (CH₂SiMe₃); 28.73, 28.33 (CHMe₂); 24.68, 23.57 (CHMe₂); 1.38 (CH₂SiMe₃). ²⁹Si NMR (39.7 MHz, C₆D₆) δ –21.50.

3.4. Preparation of (ArN)(ArNH)Mo(CH₂GeMe₃)₂–(OTf) (**6**)

The procedure was essentially the same as described above. From 1.0 g (1.41 mmol) of complex (ArN)₂Mo(CH₂GeMe₃)₂ and 0.22 g (1.41 mmol) of HOTf compound **6** was obtained as orange crystals (0.73 g, 60.0%). Anal. Calc. for C₃₃H₅₇F₃MoN₂O₃SGe₂: C, 46.04; H, 6.63. Found: C, 46.07; H, 6.63%. ¹H NMR (200 MHz,

Table 2

The details of crystallographic, collection and refinement data for **1**, **4**, **5**, **6**, **8** and **9**

	1	4	5	6	8	9
Empirical formula	C ₃₉ H ₄₅ F ₆ MoNO ₂ Si	C ₂₄ H ₃₉ F ₆ MoNO ₂ Si	C ₃₃ H ₅₇ F ₃ MoN ₂ O ₃ SSi ₂	C ₃₃ H ₅₇ F ₃ Ge ₂ MoN ₂ O ₃ S	C ₃₂ H ₅₇ ClN ₂ Si ₂ W	C ₃₂ H ₅₇ ClGe ₂ N ₂ W
Formula weight	797.79	611.59	770.99	859.99	745.28	834.28
Temperature (K)	100(2)	100(2)	293(2)	100(2) K	100(2)	100(2)
Crystal system	Monoclinic	Monoclinic	Triclinic	Triclinic	Triclinic	Triclinic
Space group	<i>P</i> 2(1)/ <i>n</i>	<i>P</i> 2(1)/ <i>c</i>	<i>P</i> $\bar{1}$	<i>P</i> $\bar{1}$	<i>P</i> $\bar{1}$	<i>P</i> $\bar{1}$
<i>a</i> (Å)	11.0593(5)	10.2681(6)	10.644(4)	10.468(4)	10.5125(5)	10.5342(5)
<i>b</i> (Å)	19.3476(9)	30.548(2)	10.694(4)	10.733(4)	11.9802(6)	12.0078(6)
<i>c</i> (Å)	18.1742(8)	10.5567(6)	18.510(6)	18.897(6)	14.6522(7)	14.7439(7)
α (°)			83.96(3)	83.40(3)	88.6150(1)	88.696(1)
β (°)	96.523(1)	117.710(1)	79.07(3)	78.51(3)	84.499(1)	84.507(1)
γ (°)			73.06(3)	71.82(3)	73.871(1)	73.760(1)
Volume (Å ³)	3863.6(3)	2931.6(3)	1976(1)	1974(1)	1764.5(2)	1782.3(2)
<i>Z</i>	4	4	2	2	2	2
<i>D</i> _{calc} (g/cm ³)	1.372	1.386	1.296	1.445	1.403	1.555
Absorption coefficient (mm ⁻¹)	0.433	0.546	0.492	1.923	3.439	4.991
<i>F</i> (000)	1648	1264	812	884	764	836
Crystal size (mm)	0.27 × 0.19 × 0.15	0.12 × 0.10 × 0.08	0.4 × 0.3 × 0.2	0.96 × 0.64 × 0.16	0.21 × 0.16 × 0.08	0.20 × 0.12 × 0.04
θ _{max} range for data collection (°)	24.25	25.00	25.05	28.00	24.50	25.00
Index ranges	-12 ≤ <i>h</i> ≤ 12, -17 ≤ <i>k</i> ≤ 22, -20 ≤ <i>l</i> ≤ 16	-12 ≤ <i>h</i> ≤ 12, -36 ≤ <i>k</i> ≤ 24, -11 ≤ <i>l</i> ≤ 12	-12 ≤ <i>h</i> ≤ 12, -12 ≤ <i>k</i> ≤ 12, -22 ≤ <i>l</i> ≤ 21	-14 ≤ <i>h</i> ≤ 13, -13 ≤ <i>k</i> ≤ 14, -13 ≤ <i>l</i> ≤ 24	-12 ≤ <i>h</i> ≤ 12, -13 ≤ <i>k</i> ≤ 13, -17 ≤ <i>l</i> ≤ 17	-8 ≤ <i>h</i> ≤ 12, -12 ≤ <i>k</i> ≤ 14, -17 ≤ <i>l</i> ≤ 17
Reflections collected	19892	16044	7406	13529	13383	9771
Independent reflections (<i>R</i> _{int})	6247 (0.0326)	5161 (0.0356)	6993 (0.0619)	9374 (0.0272)	5838 (0.0165)	6244 (0.0148)
Absorption correction				SADABS		
Max/min transmission	0.9379/0.8921	0.9576 / 0.9373	0.8956/0.7534	0.7484/0.2597	0.7705/0.5320	0.8253/0.4351
Refinement method				Full-matrix least-squares on <i>F</i> ²		
Data/restraints/parameters	6247/12/619	5161/0/472	6993/0/410	9374/0/634	5838/0/571	6244/4/571
Goodness-of-fit on <i>F</i> ²	1.038	1.003	1.018	1.006	1.038	1.038
Final <i>R</i> indices [<i>I</i> > 2σ(<i>I</i>)]	<i>R</i> ₁ = 0.0359, <i>wR</i> ₂ = 0.0907	<i>R</i> ₁ = 0.0304, <i>wR</i> ₂ = 0.0650	<i>R</i> ₁ = 0.0643, <i>wR</i> ₂ = 0.1167	<i>R</i> ₁ = 0.0400, <i>wR</i> ₂ = 0.1070	<i>R</i> ₁ = 0.0159, <i>wR</i> ₂ = 0.0386	<i>R</i> ₁ = 0.0234, <i>wR</i> ₂ = 0.0565
<i>R</i> indices (all data)	<i>R</i> ₁ = 0.0465, <i>wR</i> ₂ = 0.0948	<i>R</i> ₁ = 0.0439, <i>wR</i> ₂ = 0.0684	<i>R</i> ₁ = 0.1410, <i>wR</i> ₂ = 0.1339	<i>R</i> ₁ = 0.0458, <i>wR</i> ₂ = 0.1102	<i>R</i> ₁ = 0.0173, <i>wR</i> ₂ = 0.0391	<i>R</i> ₁ = 0.0270, <i>wR</i> ₂ = 0.0577
Largest difference peak and hole (e Å ⁻³)	1.007/−0.499	0.534/−0.226	0.637/−0.463	1.308/−1.260	0.670/−0.472	1.788/−1.072

Table 3
Selected distances (Å) and angles (°) for **1** and **4**

Distance (Å)	Angle (°)		
1			
Mo(1)–N(1)	1.725(2)	Si(1)–C(21)–Mo(1)	144.8(2)
Mo(1)–O(1)	1.910(2)	C(1)–N(1)–Mo(1)	174.83(19)
Mo(1)–O(2)	1.904(2)		
Mo(1)–C(21)	1.883(3)		
Si(1)–C(21)	1.857(3)		
4			
Mo(1)–N(1)	1.722(2)	Si(1)–C(1)–Mo(1)	138.5(1)
Mo(1)–O(1)	1.906(1)		
Mo(1)–O(2)	1.902(1)		
Mo(1)–C(1)	1.889(2)		
Si(1)–C(1)	1.862(2)		

Table 4
Selected distances (Å) and angles (°) for **5** and **6**

Distance (Å)	Angle (°)		
5			
Mo(1)–N(1)	1.925(5)	C(1)–N(1)–Mo(1)	138.2(4)
Mo(1)–N(2)	1.716(4)	C(13)–N(2)–Mo(1)	174.8(4)
Mo(1)–O(1)	2.214(4)	Si(1)–C(25)–Mo(1)	126.8(3)
Mo(1)–C(25)	2.091(5)	Si(2)–C(29)–Mo(1)	120.9(3)
Mo(1)–C(29)	2.098(5)		
Si(1)–C(25)	1.883(5)		
Si(2)–C(29)	1.880(5)		
6			
Mo(1)–N(1)	1.917(2)	C(1)–N(1)–Mo(1)	136.3(1)
Mo(1)–N(2)	1.748(2)	C(13)–N(2)–Mo(1)	175.6(1)
Mo(1)–O(1)	2.243(2)	Ge(1)–C(25)–Mo(1)	124.3(1)
Mo(1)–C(25)	2.104(2)	Ge(2)–C(29)–Mo(1)	115.9(1)
Mo(1)–C(29)	2.091(2)		
Ge(1)–C(25)	1.954(2)		
Ge(2)–C(29)	1.953(2)		

Table 5
Selected distances (Å) and angles (°) for **8** and **9**

Distance (Å)	Angle (°)		
8			
W(1)–N(1)	1.924(2)	C(1)–N(1)–W(1)	136.6(1)
W(1)–N(2)	1.755(2)	C(13)–N(2)–W(1)	176.6(1)
W(1)–Cl(1)	2.4920(5)	Si(1)–C(25)–W(1)	118.85(9)
W(1)–C(25)	2.104(2)	Si(2)–C(29)–W(1)	125.4(1)
W(1)–C(29)	2.112(2)		
Si(1)–C(25)	1.889(2)		
Si(2)–C(29)	1.887(2)		
9			
W(1)–N(1)	1.933(2)	C(1)–N(1)–W(1)	135.0(1)
W(1)–N(2)	1.745(2)	C(13)–N(2)–W(1)	176.7(1)
W(1)–Cl(1)	2.4942(6)	Ge(1)–C(25)–W(1)	122.9(1)
W(1)–C(25)	2.111(2)	Ge(2)–C(29)–W(1)	116.2(1)
W(1)–C(29)	2.093(2)		
Ge(1)–C(25)	1.973(2)		
Ge(2)–C(29)	1.976(2)		

C_6D_6) δ 9.12 (s, 1H, NH), 7.10–6.70 (m, 6H, H (3,4)), 3.93 (d, 2H, MoHCHGeMe₃, $^2J_{\text{HH}} = 8.0$), 3.64 (sept, 2H, CHMe₂), 3.53 (sept, 2H, CHMe₂), 2.68 (d, 2H,

MoHCHSiMe₃, $^2J_{\text{HH}} = 8.0$), 0.99 (d, 24H, CHMe₂, $^3J_{\text{HH}} = 6.8$), 0.40 (s, 18H, GeMe₃). ^{13}C NMR (50 MHz, C_6D_6) δ 150.75, 150.58, 148.95, 141.78, 131.05, 127.04, 124.08, 123.86 (C_{arom}); 76.94 (CH₂GeMe₃); 28.72, 28.30 (CHMe₂); 24.64, 23.52 (CHMe₂); 1.85 (CH₂GeMe₃).

3.5. Preparation of (ArN)(ArNH)W(CH₂GeMe₃)₂(OTf) (7)

To an orange solution of (ArN)₂W(CH₂GeMe₃)₂ (1.5 g, 1.90 mmol) in 15 ml of DME at –50 °C 0.30 g (2.00 mmol) of HOTf was added. The reaction mixture was stirred and allowed to warm slowly to room temperature. The solution became pale yellow-green. The solvent was removed in vacuo. The solid residue was recrystallized from of pentane to afford pale green crystals of **7** 1.13 g (65.0%). Anal. Calc. for C₃₃H₅₇F₃WN₂O₃SGe₂: C, 41.83; H, 6.06. Found: C, 41.56; H, 5.95%. ^1H NMR (200 MHz, toluene-*d*₈) δ 8.22 (s, 1H, NH), 6.90–6.70 (m, 6H, H (3,4)), 3.52 (sept, 2H, CHMe₂), 3.39 (d, 2H, WHCHGeMe₃, $^2J_{\text{HH}} = 9.0$), 2.06 (d, 2H, WHCHGeMe₃, $^2J_{\text{HH}} = 9.0$), 0.99 (d, 24H, CHMe₂, $^3J_{\text{HH}} = 6.8$), 0.37 (s, 18H, GeMe₃). ^{13}C NMR (50 MHz, toluene-*d*₈) δ 149.04, 148.93, 147.09, 142.21, 137.45, 129.74, 127.12, 123.77 (C_{arom}), 79.45 (CH₂GeMe₃, $J_{\text{C}}^{-183}\text{W} = 92.8$ Hz), 28.45, 28.26 (CHMe₂), 24.82 (CHMe₂), 2.14 (CH₂GeMe₃).

3.6. Preparation of (ArN)(ArNH)W(CH₂SiMe₃)₂(Cl) (8)

Gaseous HCl (15.8 mL, 0.71 mmol) was condensed into an orange solution of (ArN)₂W(CH₂SiMe₃)₂ (0.5 g, 0.71 mmol) in 5 ml of THF at –50 °C. The reaction mixture was stirred and allowed to warm during 1 h to room temperature. The solution became pale yellow-green. The solvent was removed in vacuo. The solid residue was recrystallized from of pentane to afford pale green crystals of **8** 0.16 g (30.0%). Anal. Calc. for C₃₂H₅₇ClN₂Si₂W: C, 51.57; H, 7.71. Found: C, 51.48; H, 7.76%. ^1H NMR (200 MHz, C_6D_6) δ 8.69 (s, 1H, NH), 7.12–6.76 (m, 6H, H (3,4)), 3.50 (sept, 2H, CHMe₂), 3.20 (d, 2H, WHCHSiMe₃, $^2J_{\text{HH}} = 9.0$), 1.75 (d, 2H, WHCHSiMe₃, $^2J_{\text{HH}} = 9.0$), 1.03 (d, 24H, CHMe₂, $^3J_{\text{HH}} = 6.8$), 0.33 (s, 18H, SiMe₃).

3.7. Preparation of (ArN)(ArNH)W(CH₂GeMe₃)₂(Cl) (9)

The procedure was essentially the same as described above. From 0.4 g (0.63 mmol) of complex (ArN)₂W(CH₂GeMe₃)₂ and 14.0 ml (0.63 mmol) of HCl gas compound **9** was obtained as pale green crystals (0.18 g, 35.0%). Anal. Calc. for C₃₂H₅₇ClGe₂N₂W: C, 46.08; H, 6.89. Found: C, 45.94; H, 6.92%. ^1H NMR (200

MHz, THF-*d*₈) δ 8.25 (s, 1H, NH), 7.40–6.60 (m, 6H, H (3,4)), 3.66 (sept, 2H, CHMe₂), 3.13 (d, 2H, WHCHGeMe₃, ²J_{HH} = 8.3), 1.80 (d, 2H, WHCH-GeMe₃, ²J_{HH} = 8.3), 1.01 (d, 24H, CHMe₂, ³J_{HH} = 6.8), 0.32 (s, 18H, GeMe₃).

3.8. Metathesis of 1-hexene

The kinetic experiments and determinations of rate constants were performed as described in the literature [11,12]. In a typical experiment to an ampule containing 1.4 mg of catalyst and connected with gas burette 0.60 g (0.85 mL) of neat 1-hexene was added in argon atmosphere. The mixture was stirred magnetically. Amount of ethylene was determined volumetrically. At appropriate time the reaction was quenched by adding of Al₂O₃ to the reaction mixture and volatiles were removed in vacuo and analyzed by GLC. The amounts of formed ethylene (determined volumetrically) and 5-decene (determined by GLC) and the rested 1-hexene (determined by GLC) were in the strong accordance.

3.9. Crystallographic data for 1, 4, 5, 6, 8 and 9

The suitable crystals of **1**, **4**, **8**, **9** for X-ray diffraction were prepared by slow evaporation of concentrated pentane solutions of the complexes at room temperature. Crystals of **5** and **6** were prepared by slow evaporation of concentrated ether solutions of the complexes at room temperature. The data were collected on a Bruker AXS “SMART APEX” diffractometer (graphite-monochromated, Mo K α -radiation, φ - ω -scan technique, $\lambda = 0.71073$ Å). The intensity data were integrated in the SAINT program [13], SADABS [14] was used to perform area-detector scaling and absorption corrections. The structures were solved by direct methods and were refined on F^2 using all reflections with SHELXTL package [15]. All non-hydrogen atoms were refined anisotropically. The hydrogen atoms in **1**, **4**, **6**, **8** and **9** were found from Fourier synthesis and refined isotropically and the H atoms in **5** (except for H(1) which was found from Fourier synthesis) were placed in calculated positions and refined in the “riding-model”. The details of crystallographic, collection and refinement data are shown in Table 2. The selected bond lengths and angles are listed in Tables 3–5.

4. Supplementary data

CCDC-273135 (**1**), -273136 (**4**), -273137 (**5**), -273138 (**6**), -273139 (**8**) and -273140 (**9**) contain the supplementary crystallographic data for this paper. These data can

be obtained free of charge at www.ccdc.cam.ac.uk/const/retrieving.html [or from the Cambridge Crystallographic Data Centre, 12 Union Road, Cambridge CB2 1EZ, UK; fax: (internat.) +44 1223 336 033; e-mail: deposit@ccdc.cam.ac.uk].

Acknowledgments

This work was supported by the Grant of President RF (Projects No. 58.2003.3 and No. 1652.2003.3) and the Russian Foundation for Basic Research (Project No. 02-03-32694). The authors thank Dr. T.I. Kulikova for GLC analysis of metathesis products.

References

- [1] L.N. Bochkarev, A.V. Nikitinskii, Y.E. Begantsova, V.I. Scherbakov, N.E. Stolyarova, I.K. Grigorieva, I.P. Malysheva, G.V. Basova, G.K. Fukin, E.V. Baranov, Yu.A. Kurskii, G.A. Abakumov, *J. Organomet. Chem.* 690 (2005) 3212.
- [2] (a) R.R. Schrock, J.S. Murdzek, G.C. Bazan, B.J. Robbins, M. DiMare, M. O'Regan, *J. Am. Chem. Soc.* 112 (1990) 3875; (b) R.R. Schrock, R.T. Depue, J. Feldman, C.J. Schaverien, J.C. Dewan, A.H. Liu, *J. Am. Chem. Soc.* 110 (1988) 1423.
- [3] R.R. Schrock, A.H. Hoveyda, *Angew. Chem., Int. Ed. Engl.* 42 (2003) 4592.
- [4] L.N. Bochkarev, A.V. Nikitinskii, A.A. Skatova, Yu.E. Begantsova, V.I. Scherbakov, I.P. Malysheva, G.V. Basova, G.K. Fukin, Yu.A. Kurskii, S.Ya. Khorshev, Yu.P. Barinova, G.A. Abakumov, *Russ. Chem. Bull., Int. Ed.* (in press).
- [5] L.N. Bochkarev, V.I. Scherbakov, I.P. Malysheva, G.V. Basova, N.E. Stolyarova, I.K. Grigorieva, A.L. Bochkarev, G.K. Fukin, Yu.A. Kurskii, G.A. Abakumov, *J. Organomet. Chem.* (in press).
- [6] R.R. Schrock, R.T. DePue, J. Feldman, K.B. Yap, D.C. Yang, W.M. Davis, L. Park, M. DiMare, M. Schofield, J. Anhaus, E. Walborsky, E. Evitt, C. Krüger, P. Betz, *Organometallics* 9 (1990) 2262.
- [7] A.V. Safronova, L.N. Bochkarev, N.E. Stolyarova, I.K. Grigorieva, I.P. Malysheva, G.V. Basova, G.K. Fukin, Yu.A. Kurskii, S.Ya. Khorshev, G.A. Abakumov, *J. Organomet. Chem.* 689 (2004) 1127.
- [8] E. Thorn-Csanyi, J.U. Zilles, *J. Mol. Catal. A* 190 (2002) 85.
- [9] L.N. Zakharov, Yu.N. Safyanov, G.A. Domrachev, *Problems Crystallochemistry (Russian edition)* (1990) 111.
- [10] M.C. Henry, J.G. Noles, *J. Am. Chem. Soc.* 82 (1960) 555.
- [11] H.H. Fox, R.R. Schrock, R. O'Dell, *Organometallics* 13 (1994) 635.
- [12] K.B. Wagener, K. Brzezinska, J.D. Anderson, T.R. Younkin, K. Steppe, W. DeBoer, *Macromolecules* 30 (1997) 7363.
- [13] Bruker SAINTPlus Data Reduction and Correction Program v. 6.02a, Bruker AXS, Madison, WI, USA, 2000.
- [14] G.M. Sheldrick, SADABS v.2.01, Bruker/Siemens Area Detector Absorption Correction Program, Bruker AXS, Madison, WI, USA, 1998.
- [15] G.M. Sheldrick, SHELXTL v. 6.12, Structure Determination Software Suite, Bruker AXS, Madison, WI, USA, 2000.